ISSN 1063-7834, Physics of the Solid State, 2017, Vol. 59, No. 7, pp. 1460–1467. © Pleiades Publishing, Ltd., 2017.
Original Russian Text © V.I. Berezkin, 2017, published in Fizika Tverdogo Tela, 2017, Vol. , No. 7, pp. 1432–1439.

FULLERENES

Charge Transfer in Carbon Composites Based on Fullerenes and Exfoliated Graphite

V. I. Berezkin

Research Center for Ecological Safety, Russian Academy of Sciences, St. Petersburg, 197110 Russia
e-mail: v.berezkin@inbox.ru

Received November 29, 2016; in final form, December 15, 2016

Abstract—Kinetic processes have been studied in composites based on fullerenes and exfoliated graphite at the initial proportions of components from 1 : 16 to 16 : 1 in mass. The samples are produced by heat treatment of initial dispersed mixtures in vacuum in the diffusion–adsorption process, their further cold pressing, and annealing. It is shown that the annealing almost does not influence the conduction mechanisms and only induces additional structural defects acting as electron traps. As a whole, the results obtained at the noted proportions of components make it possible to consider the material as a compensated metallic system with a structural disorder in which the charge transfer at temperatures from 4.2 K to room temperature is controlled by quantum interference phenomena. At low temperatures, the effect of a weak localization is observed, and the electron–electron interactions take place at medium and high temperatures.

DOI: 10.1134/S1063783417070022

1. INTRODUCTION

Carbon objects exhibit unique mechanical, optical, electronic, and other properties; because of this, they have been used on industrial scales for a long time. Their new modifications are developing continuously, which makes the materials promising for new applications in practice. By now numerous various structures and materials of natural, artificial, and synthetic origins have been designed; among these materials are porous and nonporous, monolithic, dispersed, and low-dimensional; there are various combinations of these materials to one another and also with noncarbon materials (metallic, ceramic, etc.). This variety is due to some specific features of carbon. Among them, we can note the ability to form various types of chemical bond provided by various hybridizations of atoms, to provide various characters and scales of ordering the atoms, the possibility of effective using heterogeneities of the structure at any levels (from micro- to macroscopic level) induced, for example, by introduction of impurity atoms, organization of a developed porous structure, and designing composites [1, 2].

Now, carbon materials are thought to be candidates for development of principally new materials and coatings (hardening, protective, shielding, antireflecting, and nonlinear-optical), electrical engineering components, electronic device elements, etc. In particular, structures that can be used as photodetectors, light-emitting devices, cold cathodes (field emission [3]), and superconductors have been developing.

For example, the superconductivity was obtained, as is well known [4], in fullerene structures intercalated with metals. However, these superconductors were very unstable. They quickly lost superconductivity in air because of oxidation of metallic impurities.

The synthesis technology and the properties of fullerene-based doped and undoped carbon–carbon composites were described in [5, 6]. The introduction of the sodium impurity led to the appearance of superconductivity in these materials (at temperatures $T \leq 15$ K) that was almost not affected by the air atmosphere. During synthesizing the materials, the initial mixture consisting of polycrystalline C_{60} powders, hydrocarbon binders (naphthalene $C_{10}H_8$ and other), and compounds containing doping elements were subjected to the action of high pressures and high temperatures. As a result, fullerenes and impurity elements introduced were distributed in the carbon matrix and were chemically bonded with it.

Similar undoped composites prepared by an alternate technology with applying another binder and matrix were proposed in [7]. In that work, the carbon matrix was formed using exfoliated graphite (EG), and high temperature and high pressures acted in different times. The authors measured some charge transfer parameters in these materials.

The aim of this work is to reveal the charge transfer mechanisms in the structures which were synthesized in [7]. For this purpose, their electrical and galvanomagnetic properties are studied, namely: the temperature dependences of the electrical resistivity, the mag-

netic-field dependences of the Hall coefficient and the magnetoresistance at various temperatures of the samples are measured and analyzed.

2. EXPERIMENTAL

The samples were synthesized using polycrystalline C_{60} powders and, as a binder, EG was used. The initial dispersed C_{60} + TEG mixtures were treated during a vacuum diffusion–absorption process at temperatures 550–650°C for several hours; then, they were pressed at a pressure of 0.7 GPa at room temperature ($T = T_{room}$) into ~1-mm-thick plates 13 mm in diameter. Two types of the samples were studied: annealed and unannealed. In the first case, the finished plates were annealed in vacuum (also at temperatures 550–650°C for several hours). In the second case, the plates were studied immediately after pressing. The technology was described in more detail in [7].

We fabricated the materials at nine different initial mass proportions of C_{60} and TEG, namely: C_{60} : EG = 1 : 16, 1 : 8, 1 : 4, ..., 16 : 1. For comparison, a material consisted of pure EG, i.e., without C_{60}, was fabricated also. The standard four-probe techniques were used to measure the temperature dependence of resistivity ρ in the range from $T = 4.2$ K to T_{room}; the magnetic-field dependences of Hall coefficient R_H and the magnetoresistivity $\Delta\rho/\rho = [\rho(H, T) - \rho(0, T)]/\rho(0, T)$ were measured in the range $H = 0$–25 kOe at two fixed temperatures of the samples: $T = 77$ and 300 K.

3. EXPERIMENTAL RESULTS

A preliminary analysis of the obtained data made it possible to conclude [7] that covalent bonds formed between fullerenes and the environment; the material was quite homogeneous, the character of curves $\rho(T)$, as well as the appearance of the samples were not changed.

Figure 1 shows typical dependences $\rho(T)$ observed in the annealed material. The curves correspond to the samples of pure EG (i.e., without C_{60}) and composites with relatively low, medium, and high fullerene contents. The porosity of the samples was estimated according to the technique described in [7]. It is seen that the resistivity of pure EG was minimal, and it increased with the fullerene fraction. All the samples demonstrated an increase in ρ as the measurement temperature decreased; in this case, the temperature dependence was weak: ρ changed, as an average, by a factor of almost 1.5 over the entire temperature range. The resistivity increased by the same value as a result of annealing of the samples, as was noted in [7]. The values of ρ themselves were low; in other words, the conductivity of the samples was fairly high. We call attention to the $\rho(T)$ curve shape, where some segments can be separated. At the initial segment (from $T = T_{room}$ and below), the resistivity increased relatively slowly (in Fig. 1, the dashed line shows the initial slope of the curves); then, a further decrease in the temperature led to an increase in the rate of increase in the resistivity, and the increase in ρ slowed down again at the lowest temperatures; in this case, some curves demonstrated an aspiration to a virtual constant (a constant level).

Figures 2 and 3 depict dependences $R_H(H)$ and $\Delta\rho/\rho$ for two different samples of the same composition, namely: for the unannealed and annealed C_{60} : EG = 1 : 1 samples. It is seen that coefficient R_H had a low magnitude and it was mainly positive, as well as magnetoresistance $\Delta\rho/\rho$. A similar pattern was observed in other samples. However, there are specific features in Figs. 2 and 3. So, curve *1* in Fig. 2a shows that the Hall coefficient was negative at $T = 300$ K at the initial segment and then changed its sign. In Fig. 3b, the magnetoresistance was also negative at the initial segment of curve *2*, but it became positive as the field strength increased.

4. DISCUSSION

4.1. Types and Parameters of Charge Carriers

The materials fabricated can be referred to graphite-like (sp^2-type) systems. Among these systems, as is known [1], the most perfect structure occurs in the highest quality natural graphites in which the average crystal size exceeded 50 μm.

Recall [8–11] that, at $T = T_{room}$, a single-crystal graphite has resistivity $\rho_a \approx 10^{-4}$ Ω cm along two-dimensional base layers, within which charge carriers are completely delocalized, and the resistivity across the layers $\rho_c \approx 1$ Ω cm; the charge carrier mobility is $\mu_a \approx 10^4$ cm^2 V^{-1} s^{-1}; the electron and hole concentrations are approximately the same: $n_e \approx n_h = n = (6.2–7.9) \times 10^{18}$ cm^{-3}; the ratio of the Hall mobilities $\mu_e/\mu_h = 1.09–1.12$; because of this, the Hall coefficient is small and negative, namely, $R_H \approx -5 \times 10^{-2}$ cm^3 C^{-1}. Graphite, as a whole, cannot be described as a metal, since the number of free electrons is small (~10^{-4} per atom), there are no three-dimensional metallic bonds and three-dimensionally free electrons, since the electron orbits (and electron wave functions) overlapping between neighboring layers is weak and, as a result, the band overlapping is weak (~0.04 eV) (although this overlapping exists). Because of this, the energy spectrum is semimetallic. As a result, graphite is thought to belong to compensated semimetals.

An increase in the degree of the structural disorder leads to a decrease in the microcrystallite sizes L_a; atoms in a crystal leave their sites, in which three valences become available. The vacancies capturing electrons form. With the π-electron state of lost atoms in mind, it can be expected that each of the vacancies is capable of generating up to three excess holes. Thus, the free carrier concentration increases, although their

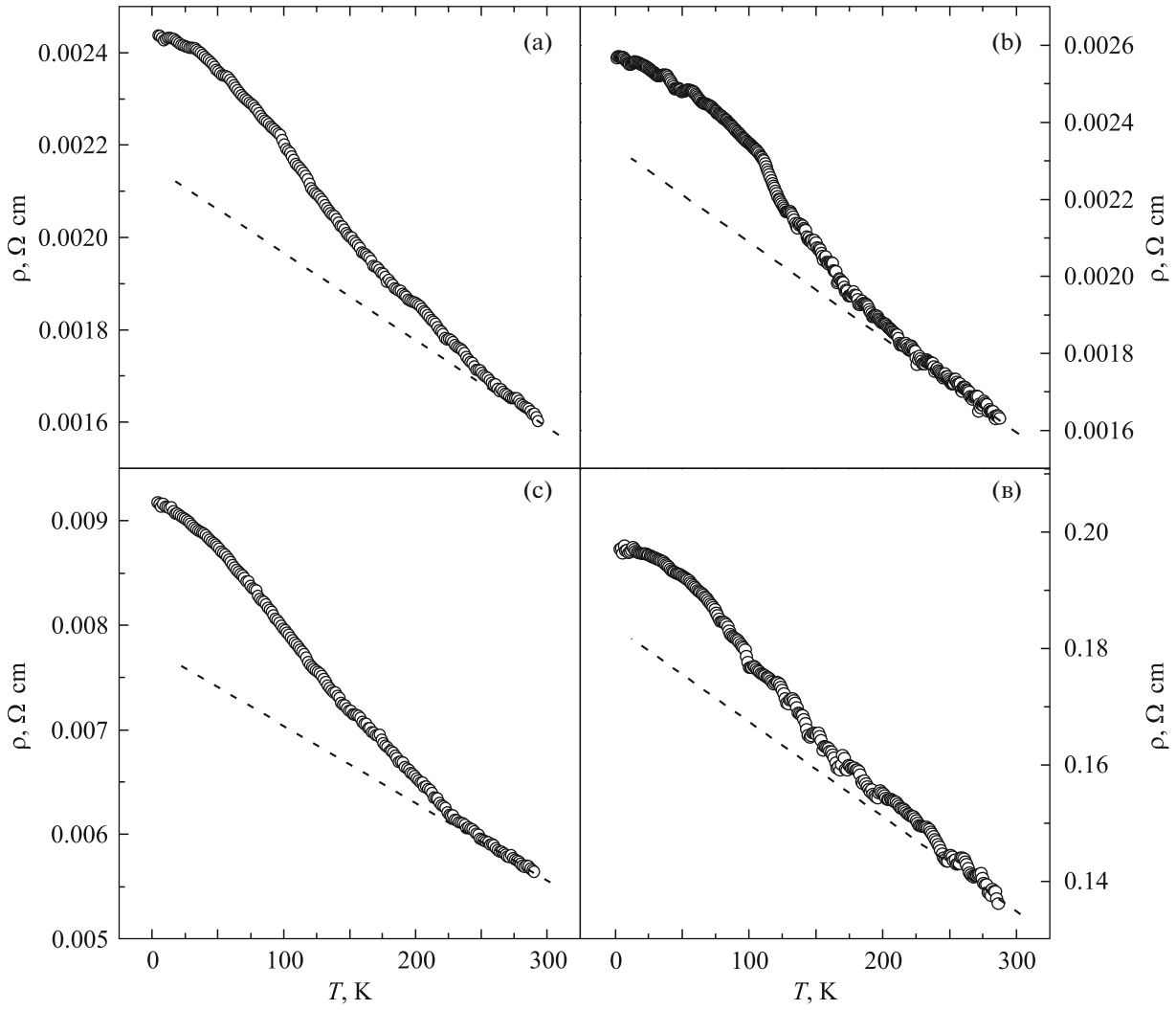

Fig. 1. Temperature dependences of the electrical resistivity of some annealed samples at different proportions of the components: (a) the sample without C_{60}, i.e., pure pressed TEG; (b) the sample with proportion C_{60} : EG = 1 : 8; (c) the C_{60} : EG = 1 : 1 sample; (d) the C_{60} : EG = 8 : 1 sample. The dashed lines show the initial (at high temperatures) the curve slope.

mobility decreases as a result of an increase in the number of defects. At L_a of ~100 nm, the bands cease to overlap; at $L_a < 100$ nm, the energy gap forms, and the Fermi level shifts down. The *n*-conductivity is transformed to the *p*-type conductivity, and the Hall coefficient changes its sign from negative to positive.

In our materials, as was mentioned previously, the Hall coefficient was mainly positive and had a small magnitude. In other words, the main carriers were holes with quite high concentration. In particular, the values of n_h estimated at $T = 77$ K and $H = 0$ were $n_h = 10.3 \times 10^{19}$, 6.3×10^{19}, and 4.2×10^{19} cm^{-3} in the annealed sample from EG without C_{60}, and the unannealed and annealed samples with the medium fullerene content (composition C_{60} : EG = 1 : 1), respectively, when using formula

$$R_H = 1/en_h, \quad (1)$$

where *e* is the electron charge. Using the expression for the conductivity

$$\sigma = 1/\rho = en_h\mu_h, \quad (2)$$

we obtained the corresponding estimations of the mobility: $\mu_h = 27$, 14, and 15 cm^2 V^{-1} s^{-1}. In other words, parameters n_h and μ_h of pure EG were higher, and the resistivity increased during annealing of the samples due to a decrease in the concentration of mobile charge carriers. It can be suggested that the annealing of the material almost did not influence the conduction mechanism (the curve shapes were not changed) but it only generated additional structural defects as a result of breaking some number of chemical bonds from the number of most tense bonds appeared during pressing of a dispersed mixture, and

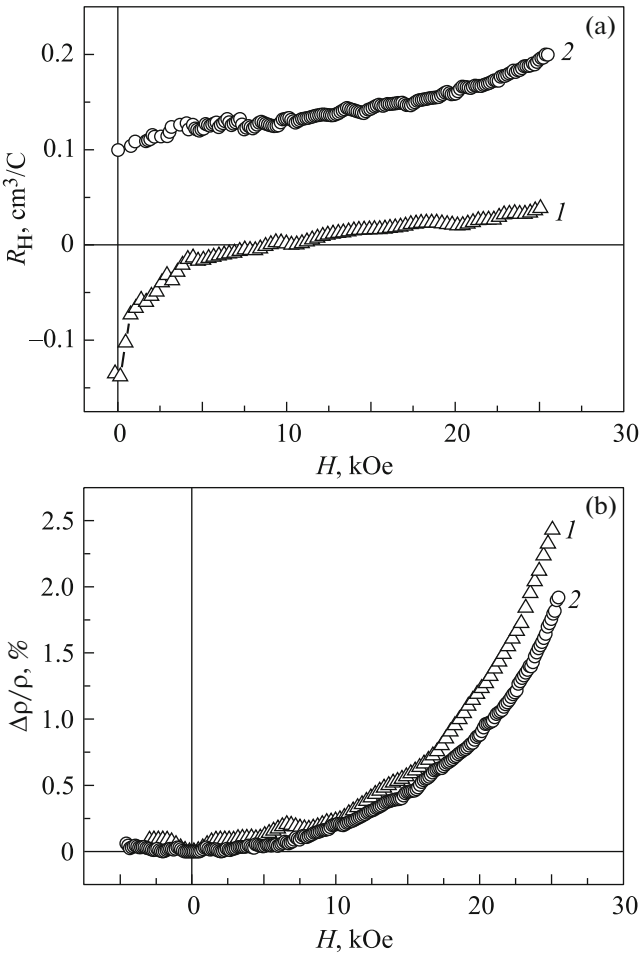

Fig. 2. Field dependences of (a) the Hall coefficient and (b) the magnetoresistance for the unannealed C_{60} : EG = 1 : 1 sample measured at (*1*) 300 and (*2*) 77 K.

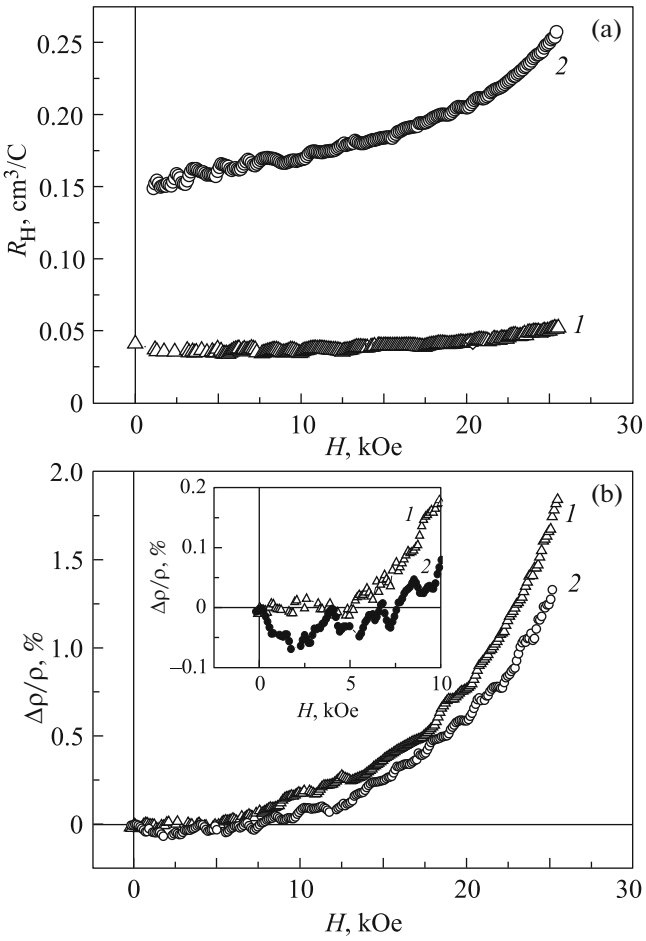

Fig. 3. Field dependences of (a) the Hall coefficient and (b) the magnetoresistance for the annealed C_{60} : EG = 1 : 1 sample measured at (*1*) 300 and (*2*) 77 K. The inset shows the initial segments of the curves shown in panel (b) in an enlarged scale.

such defects can be an additional effective channel of charge carrier capture. This assumption was confirmed by the facts as follows.

As already noted, coefficient R_H was initially negative and, then, changed its sign as the magnetic field increased, according to curve *1* in Fig. 2a. In other words, both charge carrier subsystems were manifested in the unannealed sample at $T = 300$ K; in this case, the electron subsystem was dominant in relatively weak fields, and the hole subsystem was dominant in higher magnetic fields. From the curve at $H = 0$, we found $n_e = 4.6 \times 10^{19}$ cm^{-3} and $\mu_e = 26$ cm^2 V^{-1} s^{-1}, using formulas of the types of Eqs. (1) and (2). In the case of bipolar conductivity, as is known [12], R_H is

$$R_H = \frac{A}{e}\frac{n_h\mu_h^2 - n_e\mu_e^2}{(n_h\mu_h + n_e\mu_e)^2}, \qquad (3)$$

where $A = \text{const} \approx 1$. Thus, in point $H = 9$ kOe, where $R_H = 0$, we have, according to Eq. (3), $n_h\mu_h^2 = n_e\mu_e^2$. Taking into account dependences $\sigma(T, H)$, among them, the fact that $\sigma(0) \approx \sigma(H)$, we obtained the estimation $\mu_e \approx \mu_h$ (as for $\sigma(0) \approx \sigma(H)$, we bear in mind that $\Delta\rho/\rho = 0.2\%$ at $H = 9$ kOe, according to curve *1* in Fig. 2b; therefore, the change in σ is also insignificant in this point). In other words, electrons that had higher mobility at $T = 300$ K and $H = 0$ slowed down in the magnetic field more significantly than holes did. As the temperature decreased to $T = 77$ K (curve *2* in Fig. 2a), electrons were frozen stronger than holes, and this became noticeable, since the concentrations of current carriers with different signs differed insignificantly. Thus, holes became the main current carriers at a lower temperature. In this case, the curve *2* had a "trace" of the electron subsystem as a faintly visible bend down in fields from $H \approx 5$ kOe and lower.

After annealing the sample, the dominant carriers became holes also at $T = 300$ K with parameters $n_h = 15.2 \times 10^{19}$ cm^{-3} and $\mu_h = 7$ cm^2 V^{-1} s^{-1} at $H = 0$

(Fig. 3a, curve *1*). The increase in the free hole concentration and the decrease in their mobility confirmed the assumption that the annealing led to the formation of additional electron traps which, being new structural defects, contributed also to the scattering of carriers remained free. The electron character of the trapping centers can also explain the fact of a stronger freezing of more mobile electrons. Lastly, the electron character of the trapping centers corresponded to broken covalent carbon bonds, since were characterized by an uncompensated positive charge.

We repeat that, as the temperature of the annealed sample decreased to $T = 77$ K in point $H = 0$, we had $n_h = 4.2 \times 10^{19}$ cm^{-3} and $\mu_h = 15$ cm^2 V^{-1} s^{-1} (Fig. 3a, curve *2*), i.e., the free carrier concentration decreased by a factor of almost 3.5 as compared to that obtained for $T = 300$ K, and the mobility was almost doubled. The explanation of this circumstance can be that the trapping centers became neutral after capturing electrons, and their action as scattering centers was less noticeable.

As noted above, the resistivity of the composites increased monotonically as temperature decreased; i.e., the temperature coefficient of the resistivity was negative, and the temperature dependence was weak, and neither the "semiconductor" activation law nor Mott's law for hopping conductivity were fulfilled in the $\rho(T)$ curves. All the samples had a high predominantly *p*-type conductivity, but the electron subsystem also manifested itself; in this case, the charge carrier concentration was high and their mobility was low. It can be also mentioned in Section 3 the aspiration of ρ to a constant level in some $\rho(T)$ curves at the lowest temperatures, which was characteristic of metals, since they had a finite residual conductivity $\sigma(0)$. It is also well known that the "metallic" character (*n*-type conductivity, positive temperature coefficient of the resistivity) was observed in single-crystal and nearly single-crystal graphites. In these materials, the resistivities are minimal and the charge carrier mobilities along atomic networks are very high due to the alignment of the orientations of microcrystallites whose sizes can reach tens of microns or more. Thus, all the above mentioned makes it possible to consider the composites fabricated in this work as metallic systems with a structural disorder of the type of "bad" metals or degenerate semiconductors.

As is well known (e.g., [12]), in these materials, the Hall coefficient is not dependent on field and the magnetoresistance is zero as there are carriers of a one type or they completely dominate. However, the materials under consideration contained the carriers of both the types (with different signs); because of this, dependence $R_H(H)$ took place and $\Delta\rho/\rho \neq 0$, since a magnetic field changes the contribution of various-type charge carriers to the formation of the Hall field. In these cases, in weak fields, the changes in the coefficient R_H were first due to more mobile charge carriers that could manifest themselves stronger than the less mobile carriers and, sometimes, could dominate even at relatively low intrinsic concentration. The weak-field regime was confirmed by the magnetoresistance quadratic in field, i.e., by a dependence $\Delta\rho/\rho \sim H^2$ that was observed in the experiment (Figs. 2b and 3b). As the field increased, the trajectories of more mobile current carriers, i.e., electrons, curved more and more, their contribution to the Hall field decreased, and there came a time of the change in the sign of this field (Fig. 2a, curve *1*).

It is necessary to note a noticeable role of electrons in the formation of the magnetoresistance. From the data of Figs. 2a and 3a, it follows that electrons influenced the Hall field more substantially at higher temperatures. It was clearly observed in the unannealed sample (there is a segment, where $R_H < 0$, $T = 300$ K, Fig. 2a, curve *1*). In the annealed sample, it was manifested as a lower hole concentration at $T = 300$ K than that at $T = 77$ K (Fig. 3a, curves *1* and *2*). In this situation, $\Delta\rho/\rho$ must be changed more substantially at $T = 300$ K than at $T = 77$ K, which was observed experimentally (Figs. 2b and 3b).

4.2. Shapes of Curves $\rho(T)$ and Quantum Corrections to the Conductivity

Dependences $\rho(T)$, whose shapes were similar to those shown in Fig. 1, were observed before in many carbon and noncarbon materials, such as: pyrolithic graphites [8]; Yb, at the semimetal–semiconductor phase transition (under pressure) [13]; SmB_6 [14], ultrathin superconducting granulated Pb films on SiO_2 as their thicknesses were larger than 35 Å [15]; thin (60–80 nm) films of amorphous carbon on *n*-Si substrates [3]; a high-porous biocarbon of carbonized beech wood [16], etc. Since the materials are different, the charge transfer mechanisms in them providing the characteristic shape of the $\rho(T)$ dependences are also different. For example, in Yb, these mechanisms are due to the energy band structure (unfilled *d* states); in SmB_6, e.g., they are related to the metallic conductivity in the impurity band formed by Sm vacancies.

Carbon has proper specific features. The conduction mechanism even in the same materials treated at different temperatures can be changed from the band conduction (i.e., over expanded states) to the hopping mechanism over localized states near the Fermi level, as was shown in [17]; in weakly conducting structures, the conduction can be determined even by currents limited by a space charge [18]. However, the shape of such $\rho(T)$ curves as shown in Fig. 1 was not always discussed in detail in the works on carbon.

It is generally believed that the structures closest to graphites are characterized by scattering on phonons the concentration of which decreases at low temperatures, and this is a reason why the increase in ρ slowed down in this region. The temperature variations of the

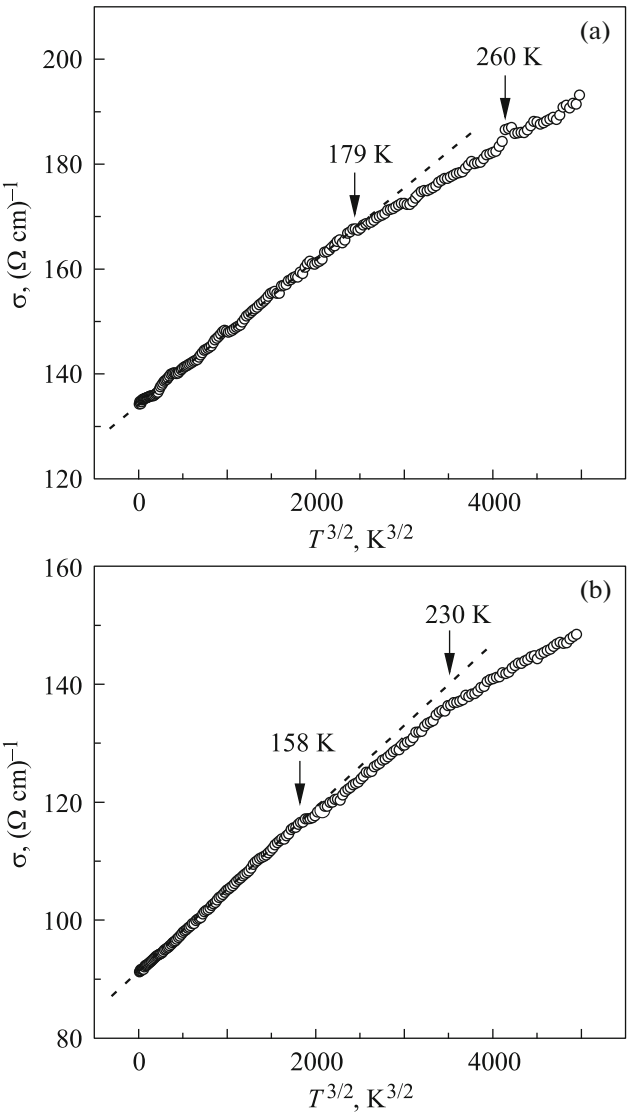

Fig. 4. Temperature dependences of the specific electrical conductivity of the C_{60} : EG = 1 : 1 samples in coordinates σ–$T^{3/2}$: (a) unannealed sample, (b) annealed sample. The dashed straight lines show the approximations of the low-temperature regions; the arrows indicate visible boundaries of different temperature segments.

conductivity in the more amorphized samples are associated with the free carrier concentration. It is implied that the resistance increases due to processes of removal free carriers as the temperature decreases. At high temperatures, the rate of increase in the resistance with the decrease in the temperature is smaller, since in this case, the phonon scattering begins to act. In the structures, in which the microcrystallite sizes in the direction of the base planes become comparable or smaller than the mean free path (that is inversely proportional to the phonon density), the role of scattering at the microcrystallite boundaries increases. In this case, the charge carrier mobility is proportional to the mean crystallite size, there is no curvature of the $\rho(T)$ dependences, i.e., they are almost horizontal straight lines with a very weak negative slope.

The feature of our dependences $\rho(T)$ was that none of them can correlate to any one law $\rho = \rho(T)$ to determine any one conduction mechanism. The segments with different characters smoothly going from one to another were observed over the entire temperature ranges. In other words, different mechanisms of charge carrier transfer and their scattering could act simultaneously.

An analysis showed that dependence $\sigma \sim T^{3/2}$ was fulfilled at low temperatures in almost all compositions; in this case, this segment had slightly different lengths along the horizontal axis in different samples. For example, this segment extended from $T = 4.2$ K to $T \approx 100$ K in the samples without C_{60} and to $T \approx 90$ K in the samples with the maximum C_{60} content. Figure 4 depicts the conductivity in the coordinates σ–$T^{3/2}$ for the unannealed and annealed samples with composition C_{60} : EG = 1 : 1. It is seen that, first, the experimental points at low temperatures fall well on the straight line and, second, the segment $\sigma \sim T^{3/2}$ in Fig. 4a ends at $T \approx 179$ K and that in Fig. 4b ends at $T \approx 158$ K.

It is well known that the law $\sigma \sim T^{3/2}$ is characteristic of nondegenerate semiconductors in the case, when charged scattering centers (usually, they are impurity ions) dominate. True, it was noted still in [19] that it is difficult to verify this law over a wide temperature range in similar materials, since the scattering by lattice vibrations (acoustic phonons, $\sigma \sim T^{-3/2}$) dominate at high temperatures, and the carriers are frozen at the impurity levels at low T, so that the ion concentration becomes exponentially dependent on temperature.

Our material must contain quite many charged centers, in particular, in the annealed samples, which was already noted in the preceding subsection. However, the composite under study was, first, a medium of the metallic type; second, the $\sigma \sim T^{3/2}$ segment extended to higher temperature ($T \approx 179$ K) than that in the annealed sample, where similar segment ended at $T \approx 158$ K. If the law $\sigma \sim T^{3/2}$ in the samples were due to the carrier scattering by charged centers, the inverse situation must be observed: the length of the segment where the law $\sigma \sim T^{3/2}$ was fulfilled must be larger in the annealed sample, since the charge center concentration in it is higher. In addition, the annealed C_{60} : EG = 1 : 1 sample has the negative magnetoresistance (Fig. 3b). It is usually observed in metallic media with a structural disorder and is interpreted in the framework of quantum interference effects [20, 21]. Note that negative magnetoresistance $\Delta\rho/\rho$ can principally be observed also due to spin effects; however, this, as is well known, requires magnetic impurities. We did not specially introduce them in the material

under study, and they existed in it randomly in trace amounts, according to the electron-probe microanalysis of the samples.

In a three-dimensional case, the temperature dependences of quantum corrections to the conductivity $\Delta\sigma(T)$ can be expressed as follows:

$$\Delta\sigma(T) = \sigma(T) - \sigma(0) = \alpha_{loc}T^{p/2} + \beta_{e-e}T^{1/2}, \quad (4)$$

where the first term in the right side is due to the effects of weak localization, and the second term appears due to the electron–electron interactions; α_{loc}, β_{e-e}, and p are coefficients. The first two coefficients are calculated for each specific material, but it is necessary to know fairly many parameters for these calculations; parameter p is determined by the mechanism of phase breaking of the wave functions of the charge carriers in their scattering.

If equation (4) is taken into account to describe our dependences $\sigma(T)$, then for the low-temperature region $p = 3$ is well suited. This is typical for phase breaking of the wave functions of charge carriers due to collisions with phonons.

As for the regions of medium and high temperatures, we failed to unambiguously interpret law $\sigma = \sigma(T)$ in all the samples, it is probable, because of simultaneous actions of several factors influencing the charge transfer processes. Along with this, two segments can be mainly distinguished in most of the samples. In particular, in Fig. 4a, these segments are at temperatures T = 179–260 K and 260 K—T_{room} and, in Fig. 4b, these segments are at temperatures T = 158–230 K and 230 K—T_{room}; in the second case, the segment boundaries are quite clearly visible even in a fine scale. These segments fall, as a rule, on the $\sigma \sim T^{1/2}$ straight line, but had different slopes. In other words, at moderate and high temperatures, the electron–electron interactions dominated the localization processes. The concentrations of phonons and electrons released from traps increase with temperature. It is likely that, at medium and high temperatures, the inelastic electron–electron interactions become more efficient from the standpoint of the phase breaking than quasi-elastic collisions between electrons and phonons.

Since dependence $T^{3/2}$ is stronger than $T^{1/2}$, it can be suggested that, at low temperatures, either coefficients α_{loc} and β_{e-e} are close in magnitude to one another or α_{loc} slightly prevails β_{e-e}. The situation is changed to the inverse that as the temperature increases; in this case the values of coefficient β_{e-e} can be different in the regions of moderate and high temperatures.

Parameters of a number of the annealed samples with different fullerene contents, T = 77 K

Parameter	Proportion C_{60} : TEG			
	–	1 : 16	1 : 1	16 : 1
C_{60} content, mass %	0	6	50	94
ρ, mΩ cm	2.28	2.58	8.06	335.73
n_h, 10^{19} cm^{-3}	10.3	6.8	4.2	0.38
μ_h, cm^2 V^{-1} s^{-1}	27.0	33.0	15.0	1.2

4.3. Effect of the Fullerene Content on the Properties of the Composites

Consider Fig. 1 again. We can note that the shapes of curves $\rho(T)$ are almost the same for all the samples (without fullerenes, with low, medium, and high fullerene contents). Because of this, it is reasonable to suppose that this specific feature is mainly determined by the carbon matrix, in which C_{60} is located, and also by the character and parameters of the technology.

The presence of fullerenes influenced the value of the resistivity of the material which was dependent on the charge carrier concentration and mobility. The table gives corresponding data for a number of the samples.

It is seen that the maximum values of the conductivity, the concentration, and the mobility were observed at a zero or minimal fullerene contents. And, referring to the edge compositions (C_{60} : EG = 1 : 16 and 16 : 1), these parameters decreased faster than the relative fraction of EG decreased (or, what is the same, the C_{60} fraction increased).

It is well known that molecular fullerene condensates themselves are weakly conducting *n*-type semiconductors with the energy gap width of 1.5–2 eV, in which ρ can reach values ~10^{14} Ω cm [22]. However, within each of C_{60} molecules, 60 π electrons are on almost completely delocalized molecular orbitals enveloping all the carbon skeleton. In other words, these electrons move almost freely in the field of 60 C^+ ions over closed trajectories, and here, unlike graphite systems, about free holes, of course, there can be no question. Because of this, the compensation effects are possible as such electrons take part in through currents over the common C_{60} + EG structure. The compensation effects will take place at the condition that C_{60} molecules (or their small blocks) have covalent bonds with the carbon matrix, which was confirmed experimentally [7]. In the case of through currents, the structural defects in such a common system, besides the intrinsic defects of the pressed EG and uncontrolled impurities, will be pentagons in fullerene skeletons and the chemical bonds of various types connecting the C_{60} molecules to one another and with the matrix.

At the noted circumstances, the compensation effects can be amplified as the fullerene content increased, and the mean time between elementary acts of scattering of free charge carriers can decrease. In other words, a decrease in the measured concentrations and the mobilities of charge carriers can be faster than the decrease in the EG fraction in the material, which was observed in the experiment.

5. CONCLUSIONS

We studied the kinetic processes in proposed before carbon composites based on fullerenes and exfoliated graphite at nine initial proportions C_{60} : EG = 1 : 16, 1 : 8, 1 : 4, ..., 16 : 1 in mass. The samples were fabricated by heat treatment in vacuum during the diffusion–absorption process of the initial dispersed mixtures at temperatures 550–650°C for several hours, their further cold pressing, and annealing.

The revealed parameters of the processes and the observed effects made it possible to consider these materials as graphite systems of the type of "bad" metals or highly doped (degenerate) semiconductors.

The main charge carriers were holes, traditional for graphite-like systems, but electrons also manifested themselves.

The annealing of the material almost did not influence the conduction mechanisms; it only induced additional structural defects. This was likely, due to breaking of several amount of chemical bonds from the most tense bonds appeared during pressing of a dispersed mixture. Such defects played a role of trapping centers as an additional effective channel of capturing free electrons.

The charge transfer was controlled by quantum interference phenomena; in this case, the weak localization effects were more noticeable at low temperatures and the electron–electron interactions at medium and high temperatures.

The maximum values of the conductivity, the concentration and the mobility were observed in the pure pressed TEG and in the composite with minimal fullerene content. As the C_{60} concentration increased, these parameters decreased faster than it can be expected, which can be explained as an enhancement of the compensation effects and the decrease in the mean relaxation time of free charge carrier scattering.

ACKNOWLEDGMENTS

The author is grateful to V.V. Popov for useful discussions.

REFERENCES

1. V. I. Berezkin, *Carbon: Closed Nanoparticles, Macrostructures, Materials* (ARTEGO, St. Petersburg, 2013) [in Russian].
2. V. I. Berezkin, *Introduction to Physical Adsorption and Technology of Carbon Adsorbents* (Viktoriya Plyus, St. Petersburg, 2013) [in Russian].
3. Q. Z. Xue and X. Zhang, Carbon **43**, 760 (2005).
4. O. Gunnarson, Rev. Mod. Phys. **69**, 575 (1997).
5. V. I. Berezkin, JETP Lett. **83**, 388 (2006).
6. V. I. Berezkin and V. V. Popov, Phys. Solid State **49**, 1803 (2007).
7. V. I. Berezkin, V. V. Popov, and M. V. Tomkovich, Phys. Solid State **59**, 620 (2017).
8. C. A. Klein, Rev. Mod. Phys. **34**, 56 (1962).
9. *Short Chemical Encyclopedy,* Ed. by I. L. Knunyants (Sov. Entsiklopediya, Moscow, 1967), Vol. 5 [in Russian].
10. M. S. Dresselhaus and G. Dresselhaus, Adv. Phys. **30**, 139 (1981).
11. S. V. Shulepov, *Physics of Carbon-Graphite Materials* (Metallurgiya, Chelyabinsk, 1990) [in Russian].
12. P. S. Kireev, *Semiconductor Physics* (Vysshaya Shkola, Moscow, 1975, Mir, Moscow, 1978).
13. D. B. McWhan, T. M. Rice, and P. H. Schmidt, Phys. Rev. **177**, 1063 (1969).
14. J. C. Nickerson, R. M. White, K. N. Lee, R. Bachmann, T. H. Geballe, and G. W. Hull, Jr., Phys. Rev. B **3**, 2030 (1971).
15. H. M. Jaeger, D. B. Haviland, B. G. Orr, and A. M. Goldman, Phys. Rev. B **40**, 182 (1989).
16. L. S. Parfen'eva, T. S. Orlova, N. F. Kartenko, N. V. Sharenkova, B. I. Smirnov, I. A. Smirnov, H. Misiorek, A. Jezowski, T. E. Wilkes, and K. T. Faber, Phys. Solid State **52**, 1115 (2010).
17. V. V. Popov, T. S. Orlova, E. Enrique Magarino, M. A. Bautista, and J. Martinez-Fernandez, Phys. Solid State **53**, 276 (2011).
18. I. Lazar and G. Lazar, J. Non-Cryst. Solids **352**, 2096 (2006).
19. K. Seeger, *Semiconductor Physics* (Springer, Wien, New York, 1973).
20. B. I. Altshuler and A. G. Aronov, in *Electron-Electron Interactions in Disordered Systems,* Vol. 10 of *Modern Problems in Condensed Matter Science,* Ed. by A. L. Efros and M. Pollak (North-Holland, Amsterdam, 1985), p. 1.
21. P. A. Lee and T. V. Ramakrishnan, Rev. Mod. Phys. **57**, 287 (1985).
22. T. L. Makarova, Semiconductors **35**, 243 (2001).

Translated by Yu. Ryzhkov